Lineage-specific compaction of *Tcrb* requires a chromatin barrier to protect the function of a long-range tethering element

Kinjal Majumder,[1] Olivia I. Koues,[1] Elizabeth A.W. Chan,[2] Katherine E. Kyle,[1] Julie E. Horowitz,[3] Katherine Yang-Iott,[3] Craig H. Bassing,[3] Ichiro Taniuchi,[4] Michael S. Krangel,[2] and Eugene M. Oltz[1]

[1]Department of Pathology and Immunology, Washington University School of Medicine in St. Louis, St. Louis, MO 63110
[2]Department of Immunology, Duke University Medical Center, Durham, NC 27710
[3]Division of Cancer Pathobiology, Department of Pathology and Laboratory Medicine, Center for Childhood Cancer Research, The Children's Hospital of Philadelphia and Abramson Family Cancer Research Institute, Perelman School of Medicine, University of Pennsylvania, Philadelphia, PA 19104
[4]Laboratory for Transcriptional Regulation, RIKEN Center for Integrative Medical Sciences, Yokohama, Kanagawa 230-0045, Japan

Gene regulation relies on dynamic changes in three-dimensional chromatin conformation, which are shaped by composite regulatory and architectural elements. However, mechanisms that govern such conformational switches within chromosomal domains remain unknown. We identify a novel mechanism by which cis-elements promote long-range interactions, inducing conformational changes critical for diversification of the TCRβ antigen receptor locus (*Tcrb*). Association between distal Vβ gene segments and the highly expressed DβJβ clusters, termed the recombination center (RC), is independent of enhancer function and recruitment of V(D)J recombinase. Instead, we find that tissue-specific folding of *Tcrb* relies on two distinct architectural elements located upstream of the RC. The first, a CTCF-containing element, directly tethers distal portions of the Vβ array to the RC. The second element is a chromatin barrier that protects the tether from hyperactive RC chromatin. When the second element is removed, active RC chromatin spreads upstream, forcing the tether to serve as a new barrier. Acquisition of barrier function by the CTCF element disrupts contacts between distal Vβ gene segments and significantly alters *Tcrb* repertoires. Our findings reveal a separation of function for RC-flanking regions, in which anchors for long-range recombination must be cordoned off from hyperactive RC landscapes by chromatin barriers.

CORRESPONDENCE
Eugene M. Oltz:
eoltz@wustl.edu

Abbreviations used: 3C, chromosome conformation capture; 3D, three-dimensional; AgR, antigen receptor; BAC, bacterial artificial chromosome; ChIP, chromatin immunoprecipitation; DN, double negative; DP, double positive; FISH, fluorescent in situ hybridization; RC, recombination center.

The packaging of mammalian genomes into chromatin and its folding into discrete topological domains can be altered dynamically to regulate gene expression. In many cases, these processes are linked mechanistically. For example, conversion of repressive to active chromatin is usually preceded by changes in locus topology that facilitate long-range contacts between gene promoters and their regulatory elements, including transcriptional enhancers (Sanyal et al., 2012; de Laat and Duboule, 2013). Deciphering the regulatory logic that sets active and inactive conformations within a genomic space to control expression of its composite genes remains an important goal.

In this regard, antigen receptor (AgR) loci serve as models to study the relationships between regulatory elements and developmental alterations of chromatin, three-dimensional (3D) conformation, and gene activity (Cobb et al., 2006; Jackson and Krangel, 2006; Jhunjhunwala et al., 2008; Steinel et al., 2010). In precursor lymphocytes, specific regions within AgR loci are activated and then repressed at distinct stages of development (Osipovich and Oltz, 2010). Dynamic changes in chromatin and locus topology direct the ordered assembly of immunoglobulin (*Ig*) and T cell receptor (*Tcr*) genes from large arrays of variable (V), diversity (D), and joining

The Rockefeller University Press $30.00
J. Exp. Med. 2015 Vol. 212 No. 1 107–120
www.jem.org/cgi/doi/10.1084/jem.20141479

(J) segments. Although each step in the assembly process is executed by a common enzymatic machinery, composed of the RAG1 and RAG2 proteins, recombination is initiated only within regions of AgR loci marked by accessible chromatin (Cobb et al., 2006). Moreover, recombination between distant gene segments requires their spatial apposition via locus contraction (Kosak et al., 2002; Skok et al., 2007).

The general architecture of AgR loci and the mechanisms used to control their assembly share many similarities (Shih and Krangel, 2013). As an example, thymocytes first activate an enhancer, termed Eβ, situated at the 3′ terminus of the 700-kb *Tcrb* locus (Bories et al., 1996; Bouvier et al., 1996). Once activated, Eβ interacts with promoters flanking two clusters of DβJβ gene segments, forming stable loops and triggering transcription of the unrearranged segments (Oestreich et al., 2006). The germline transcription is accompanied by covalent modification and opening of chromatin, which attracts RAG-1/2 binding and mediates Dβ to Jβ recombination (Ji et al., 2010b). Indeed, robust germline transcription at (D)J clusters is an initial activation event at all AgR loci, which generates a focal zone of RAG binding, termed the recombination center (RC; Schatz and Ji, 2011). At *Tcrb*, DβJβ joins serve as substrates for long-range recombination with an array of 30 *Trbv* segments that are separated from the RC by 250–500 kb. Analogous to other AgR loci, long-range *Tcrb* recombination requires lineage-specific changes in locus topology. Upon commitment to the T cell lineage, the entire locus contracts, bringing distal *Trbv* segments into spatial proximity with the RC (Skok et al., 2007). In addition to the global "contraction," which brings the locus ends together, the *Trbv* cluster itself adopts a more densely packed configuration in thymocytes. This more compact configuration likely facilitates efficient sampling of Vβ gene segments by the RC after locus contraction, ensuring a diverse *Trbv* repertoire.

Recent studies have begun to reveal the cis-elements and trans-acting factors that underlie some topological changes at AgR loci. A common theme is the involvement of CTCF and the cohesin complex, which together play a major role in sculpting the 3D architecture of eukaryotic genomes (Phillips and Corces, 2009). CTCF binds directly to DNA at thousands of genomic sites, which can interact through space via CTCF-CTCF dimerization. These contacts are stabilized by CTCF-mediated recruitment of cohesin, which forms a collar around the base of resultant chromatin loops (Nasmyth and Haering, 2009). In developing lymphocytes, ablation of CTCF or RAD21, a critical cohesin subunit, impairs promoter-enhancer interactions and perturbs the repertoire of distant V segments used in long-range V(D)J recombination (Ribeiro de Almeida et al., 2011; Seitan et al., 2011). In addition to its structural role, CTCF regulates AgR assembly via its insulator function, forming boundaries between active and repressive chromatin domains. At both *Igh* and *Igk*, CTCF-bound insulators prevent the spread of active chromatin from the RC to the most proximal V gene segments (Guo et al., 2011b; Xiang et al., 2013). Inactivating mutation of these elements augments germline transcription and recombination of the most RC-proximal V segments, presumably by extending the reach of powerful enhancers situated in the RC. In what may be a related finding, all of these CTCF-binding elements associate by contact with the collection of enhancers that decorate the 3′ end of the *Igh*- and *Igk*-RCs (Guo et al., 2011b; Xiang et al., 2013).

Although the roles of CTCF-bound regions in AgR locus conformation are emerging, the requirements for transcriptional regulatory elements in these lineage-specific processes remain murky. Conflicting data exist for whether *Ig* and *Tcr* enhancers are required for contraction of their corresponding loci (Guo et al., 2011a; Shih et al., 2012; Medvedovic et al., 2013). With regard to the more intricate aspects of AgR locus topology, enhancer deletions consistently disrupt their associations with distal promoters and other enhancers (Shih and Krangel, 2013). However, existing data derive from the perspective of regulatory elements rather than monitoring specific interactions between V and (D)J clusters. We now probe multiple perspectives to determine how promoters and enhancers within the *Tcrb*-RC shape its active, lineage-specific conformation. In thymocytes, we find that the large *Trbv* array is juxtaposed with the RC independent of enhancer function, RAG binding, and germline transcription. Instead, the active *Tcrb* conformation depends on an RC-flanking region, which harbors a chromatin barrier function but is not the major contact point for *Trbv* segments. Loss of the RC-proximal region activates a nearby CTCF-binding site to become a new chromatin barrier, disarming it as the major contact point for distal *Trbv* segments. Our findings indicate a separation of function for RC-flanking regions, which require that long-range contact points be insulated from the hyperactive landscape of the RC.

RESULTS

RC activation is dispensable for its long-range interactions with *Trbv*

The molecular determinants for spatial apposition of distal *Trbv* segments with their DβJβ targets remain unknown. A key RC feature is its robust, Eβ-dependent transcriptional activity, which decorates the DβJβ clusters with H3K4me3 and RAG-1/2 (Ji et al., 2010a,b). As proposed by others, this molecular landscape may be a prerequisite for capturing distant *Trbv* segments into a transcription factory occupied by the highly expressed RC, forming long-range *Tcrb* loops (Verma-Gaur et al., 2012). Accordingly, inactivation of the RC should exclude it from transcription factories and disrupt long-range V-DJ interactions. Prior studies at *Igh* and *Igk* suggest that distant V-RC interactions are enhancer independent (Hewitt et al., 2008; Medvedovic et al., 2013), but these conclusions are complicated by residual RC transcription and potential redundancies between multiple enhancers. In contrast, deletion of Eα cripples transcription of the *Tcra*-RC and perturbs its interactions with proximal *Trav* segments (Shih et al., 2012). As such, the validity of the transcription factory co-occupancy model remains unresolved.

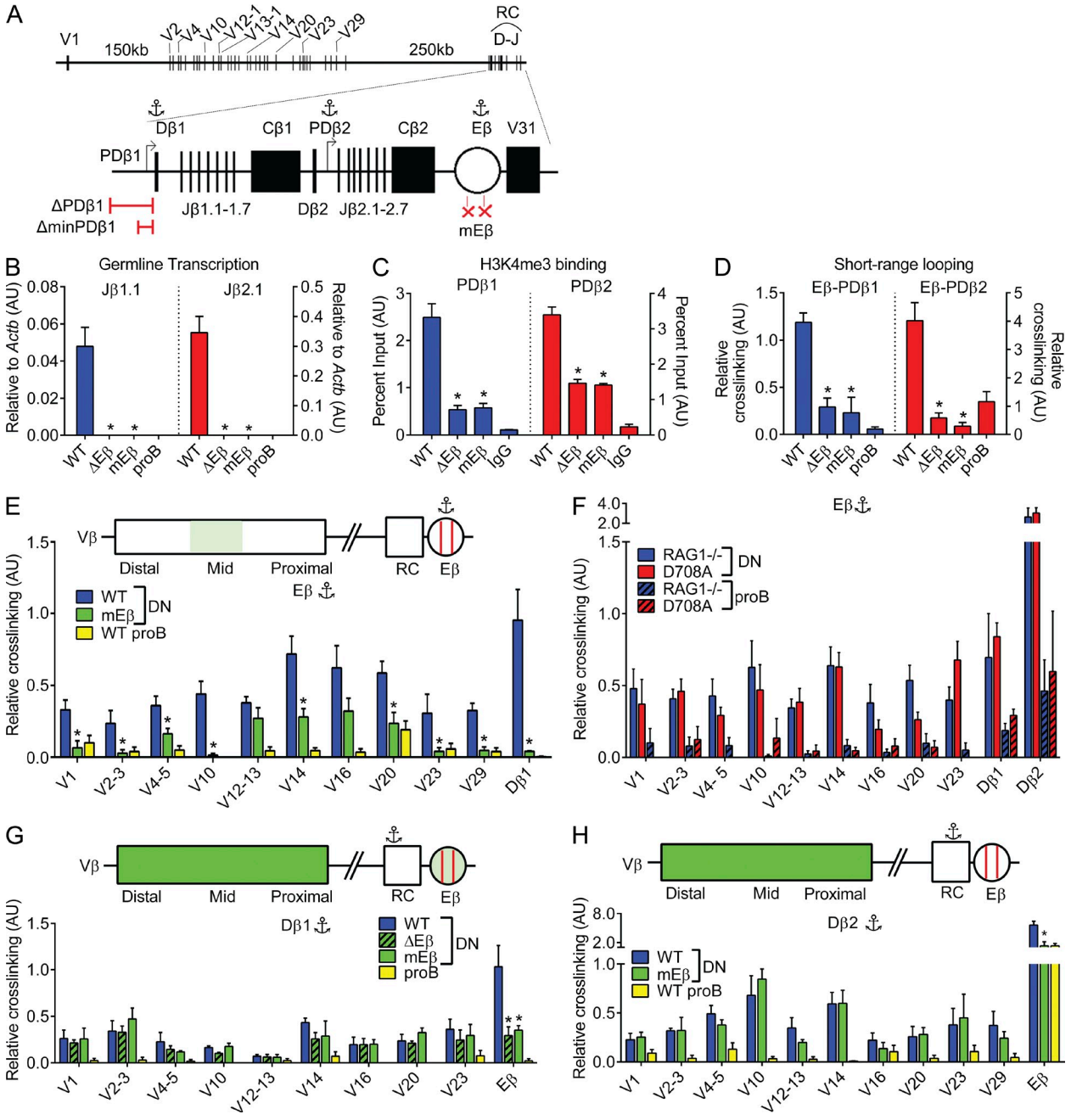

Figure 1. Long-range *Trbv*–RC interactions are Eβ independent. (A) Schematic depiction of the entire mouse *Tcrb* locus (top) and a magnified version of 30 kb spanning the RC (bottom). Promoter deletions (ΔPDβ1 and ΔminPDβ1) and enhancer mutations (mEβ) are shown at the bottom. Viewpoints used in 3C assays are designated as anchor symbols. (B) Germline transcription was measured relative to *Actb* in RAG-deficient thymocytes (WT, mEβ, or ΔEβ alleles) and pro-B cells (B220$^+$ cells from RAG1$^{-/-}$ bone marrow) as described previously (Osipovich et. al, 2007). (C) H3K4me3 deposition was measured by ChIP at PDβ1 and PDβ2 in RAG-deficient thymocytes (WT, mEβ, or ΔEβ alleles). ChIP using a nonspecific isotype control is shown (IgG). (D) 3C analysis was performed to test the cross-linking between Eβ and Dβ1 (left) or Dβ2 (right) in RAG-deficient thymocytes (WT, mEβ, or ΔEβ alleles) and pro-B cells (background levels). (E) Long-range interactions were tested by 3C using the Eβ viewpoint (anchor symbol). Relative cross-linking between HindIII fragments spanning Eβ and each indicated gene segment was calculated as described previously (Gopalakrishnan et al., 2013). The data are summarized as a cartoon in the top. Green shading indicates whether cross-linking in mEβ relative to WT alleles is unchanged (darkest green), reduced significantly (lighter green), or reduced to background levels in pro-B cells (white). (F) 3C assays were performed with the Eβ viewpoint (anchor) in DN thymocytes and pro-B cells from RAG-deficient mice, either lacking or expressing a D708A RAG transgene (Ji et al., 2010b). (G) 3C assays were performed with the Dβ1 viewpoint (anchor) in DN thymocytes (WT, Eβ, or ΔEβ alleles) and pro-B cell controls. Results are summarized in the schematic on top as described in E. (H) 3C interactions were monitored using the Dβ2 viewpoint (anchor). Data are presented as mean values from at least three independent experiments (±SEM). Thymocytes were pooled from 5–10 mice per experiment. Each panel shows data from independent experiments performed in triplicate. Significant differences between WT and mEβ samples are denoted as *, $P < 0.05$ (Student's *t* test).

Mouse *Tcrb* harbors a single known enhancer that is essential for transcription and recombination of its RC in double-negative (DN) thymocytes (Bories et al., 1996; Bouvier et al., 1996). When transcriptionally active, the *Tcrb*-RC samples Vβ segments by adopting a thymocyte-specific conformation, in which these distal elements are brought into spatial proximity (Gopalakrishnan et al., 2013). To directly test causal relationships between RC activation and *Trbv*-DβJβ associations, we measured their spatial proximity in DN thymocytes containing transcriptionally active or inactive versions of DβJβ clusters. Thymocytes with a transcriptionally inactive RC derive from mice in which two critical Runx-binding sites in Eβ were destroyed by targeted mutagenesis (Fig. 1 A, mEβ). The mutant Eβ maintains linear spacing within the RC but recapitulates all aspects of *Tcrb* inactivation observed with a complete Eβ deletion, termed ΔEβ (Mathieu et al., 2000). The defects resulting from enhancer inactivation include ablation of germline DβJβ transcription (Fig. 1 B), diminished levels of H3K4me3 deposition (Fig. 1 C), and loss of looping between the enhancer region and both Dβ-associated promoters (Fig. 1 D). Unless indicated otherwise, DN thymocytes for all experiments were from mice bred into a RAG1-deficient background (C57BL/6) to preclude *Tcrb* rearrangements, which would confound interpretation of looping data.

We measured *Trbv*-RC association in WT versus mEβ alleles using chromosome conformation capture (3C), which quantifies cross-linking efficiency of a given genomic viewpoint with other restriction fragments (Dekker et al., 2002). As shown in Fig. 1 E, the Eβ region associates more efficiently with *Trbv* segments in DN thymocytes compared with pro-B cells, confirming its cell type–specific interactome (Gopalakrishnan et al., 2013). No significant differences are observed for long-range *Tcrb* interactions in DN thymocytes from RAG1-deficient mice compared with those expressing a catalytically inactive, but binding-competent version of RAG1 (D708A; Fig. 1 F; Ji et al., 2010b). Thus, DN-specific looping between the Vβ cluster and *Tcrb*-RC is independent of RAG1 binding.

Interactions between the enhancer region and *Trbv* segments are mostly diminished in DN thymocytes from mEβ animals (Fig. 1 E). However, the inactive Eβ maintains a subset of contacts with the central *Trbv12-Trbv16* cluster (see Discussion). Surprisingly, associations between *Trbv* segments and both DβJβ clusters within the RC are unaffected by deletional or mutational inactivation of the enhancer when monitored from either Dβ viewpoint (Fig. 1, G and H). Thus, when Eβ is functional, it interacts with RC promoters and incorporates into the *Trbv*-DJ interactome; but when this enhancer is disabled, it separates from the thymocyte-specific aggregation of VDJ gene segments. We conclude that *Tcrb* adopts a thymocyte-specific conformation, which facilitates long-range *Trbv*-DJ interactions, independent of Eβ function, RC transcription, and RAG deposition. Importantly, these findings formally preclude the transcription factory co-occupation model for *Tcrb* looping.

Trbv topology and transcription is largely Eβ independent

By comparison with cells from other lineages, the *Trbv* cluster adopts a more compact conformation in DN thymocytes (Skok et al., 2007), which likely facilitates sampling of *Trbv* segments by the RC and diversifies their usage in the primary TCRβ repertoire. However, recombination of *Trbv* segments is not completely normalized; instead, it is influenced significantly by relative levels of Vβ germline transcription (Gopalakrishnan et al., 2013). Thus, the primary TCRβ repertoire is determined by both topological and transcriptional properties of the *Trbv* cluster.

To assess whether Eβ is required for these repertoire-sculpting features, we measured intra-Vβ association using 3C. When examined from viewpoints in either the distal (*Trbv5*) or proximal (*Trbv23*) portion of the cluster, intra-*Trbv* cross-linking is unaffected by the mEβ mutation (Fig. 2, A and B). However, in keeping with data presented in Fig. 1, long-range association of *Trbv5* and *Trbv23* with the enhancer is reduced. In mEβ thymocytes, both CTCF and RAD21 remain bound to sites within *Tcrb* at levels well above background; their binding differed statistically at only one tested site in the *Trbv* cluster, *Trbv10*, where CTCF decreased modestly (Fig. 2, C and D). However, inactivation of Eβ diminished transcription at a subset of *Trbv* segments that are most highly expressed in DN thymocytes (Fig. 2 E). Attenuated expression of these germline segments may reflect either a requirement for association with a transcriptionally active RC or with the functional Eβ element (see Discussion). We conclude that Eβ is dispensable for compaction of the *Trbv* cluster but augments the transcriptional activity of specific Vβ segments, which could influence the primary *Tcrb* repertoire. A definitive test is precluded because Eβ is essential for DβJβ recombination, a prerequisite for subsequent rearrangement of *Trbv* segments.

RC promoter deletion reveals two *Trbv* interaction domains

In addition to Eβ, transcription and rearrangement of the RC is controlled by two promoters, termed PDβ1 and PDβ2, situated within their respective DβJβ clusters (Fig. 1 A; Sikes et al., 1998, 2002). Activation of the Dβ1Jβ, but not Dβ2Jβ, cluster is crippled in thymocytes harboring a 3.5-kb deletion spanning PDβ1 (ΔPDβ1 allele; Fig. 1 A; Whitehurst et al., 1999). To test whether activities associated with the promoter region contribute to folding of *Tcrb* into its active conformation, we performed 3C analyses on DN thymocytes from ΔPDβ1/*Rag1*$^{-/-}$ mice. Because ΔPDβ1 removes one relevant restriction site near Dβ1, we focused RC interactome experiments on Dβ2 and Eβ. As shown in Fig. 3 A (top), Dβ2 interactions with the most proximal portion of the *Trbv* cluster are unaffected by the ΔPDβ1 mutation (*Trbv16-30*). However, we observe a significant reduction in Dβ2 cross-linking with distal portions of the *Trbv* array (*Trbv1-14*). Precisely the same bifurcation in long-range interactions is observed when Eβ is used as the 3C viewpoint (Fig. 3 B). The ΔPDβ1 mutation also reduced CTCF levels at sites in the distal *Trbv* array (Fig. 3 C), which may be a consequence of disrupting their

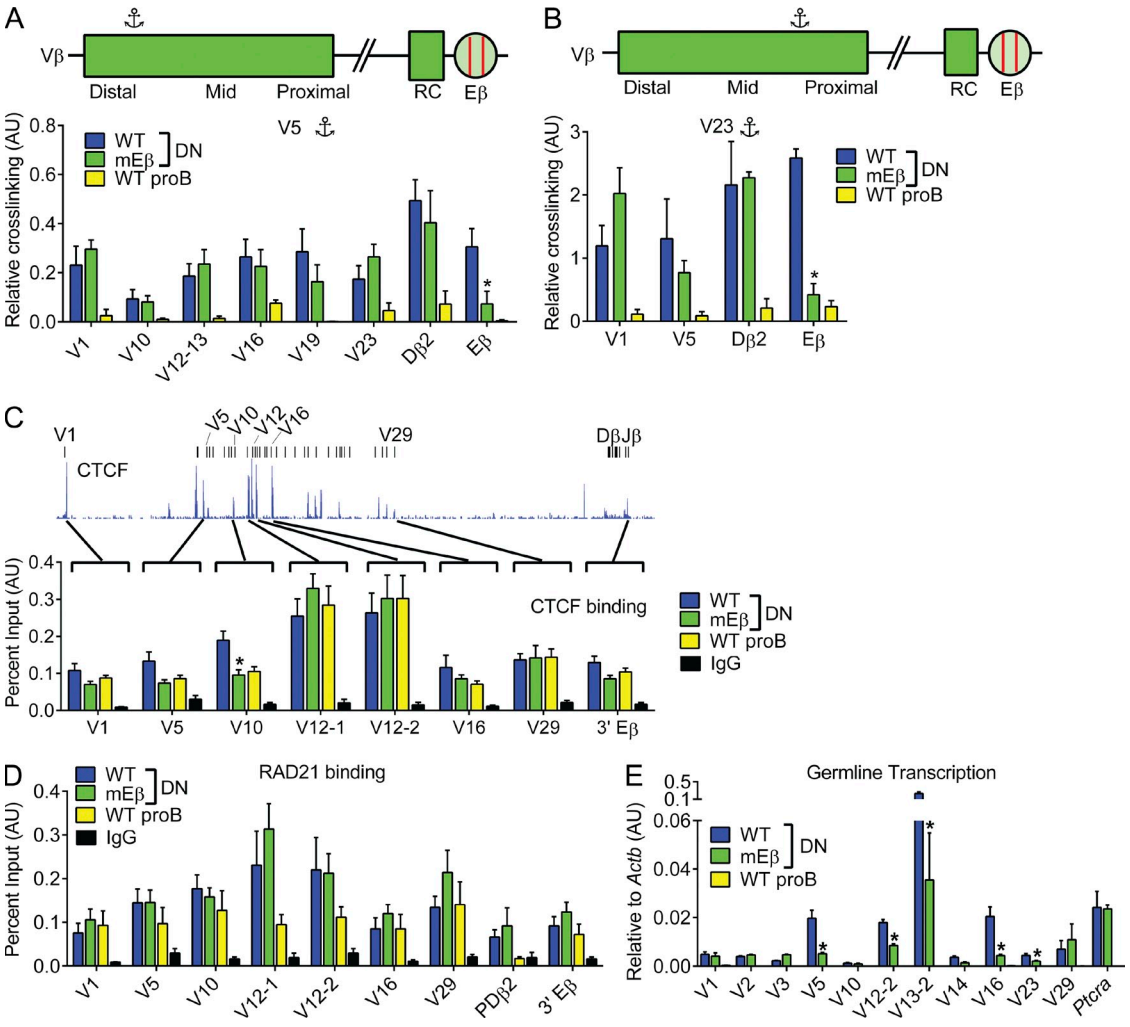

Figure 2. Impact of Eβ on topology, structural protein deposition, and transcription of Vβ segments. (A and B) Schematics and histograms of 3C data for the *Trbv5* (A) and *Trbv23* (B) viewpoints (anchors) in RAG-deficient DN thymocytes or pro-B cells (see Fig. 1 A for details). (C) Published ChIP-seq profile for CTCF in RAG-deficient DN thymocytes (top; Shih et al., 2012). (C and D) ChIP-qPCR for CTCF (C) and RAD21 (D) binding at the indicated sites in WT or mEβ thymocytes versus RAG-deficient pro-B cells. Data are presented as mean values for percent input signal from at least three independent experiments (±SEM). (E) Germline transcription of *Trbv* segments as monitored by RT-qPCR assays in the indicated cell types. Mean values from three independent experiments after normalization to signals for *Actb* are shown (±SEM). Thymocytes were pooled from 5–10 mice per experiment. Significant differences between WT and mEβ samples are denoted as *, $P < 0.05$ (Student's *t* test).

association with CTCF-rich elements near the RC (see Discussion). However, RAD21 binding and germline *Trbv* transcription throughout *Tcrb* are unaffected in ΔPDβ1 thymocytes (Fig. 3, D and E).

To gain more insight into its putative bidomainal structure, we probed interactomes of the *Trbv* array using a distal and a proximal Vβ segment as viewpoints. The distal *Trbv5* segment exhibits tissue-specific, enhancer-independent association with other gene segments in the *Trbv* array, as well as a robust interaction with the RC (Fig. 3 A, bottom). Crosslinking of this region with other distal Vβ segments is unaffected by the ΔPDβ1 deletion. However, its associations with the proximal half of *Trbv* and with the RC are significantly diminished in ΔPDβ1 thymocytes. Thus, the more distal *Trbv* segments form a higher-order structure independent of PDβ1 but require this promoter region for its interaction with the 3′ half of the *Trbv* cluster. Conversely, the more proximal *Trbv23* region associates with the RC and another 3′ segment, *Trbv29*, independent of PDβ1 but requires this promoter region for its association with more distal *Trbv* segments (Fig. 3 F).

A primary function of the region deleted from ΔPDβ1 alleles is promoter activity, which drives transcription and remodels the Dβ1Jβ chromatin landscape (Whitehurst et al., 1999). To explore whether promoter function is the primary determinant of long-range interactions between distal *Trbv* segments and the RC, we revived a mouse strain that harbors a deletion spanning only the minimal promoter upstream of Dβ1 (ΔminPDβ1; Whitehurst et al., 2000). Only residual levels of germline Dβ1 transcription are detected in thymocytes

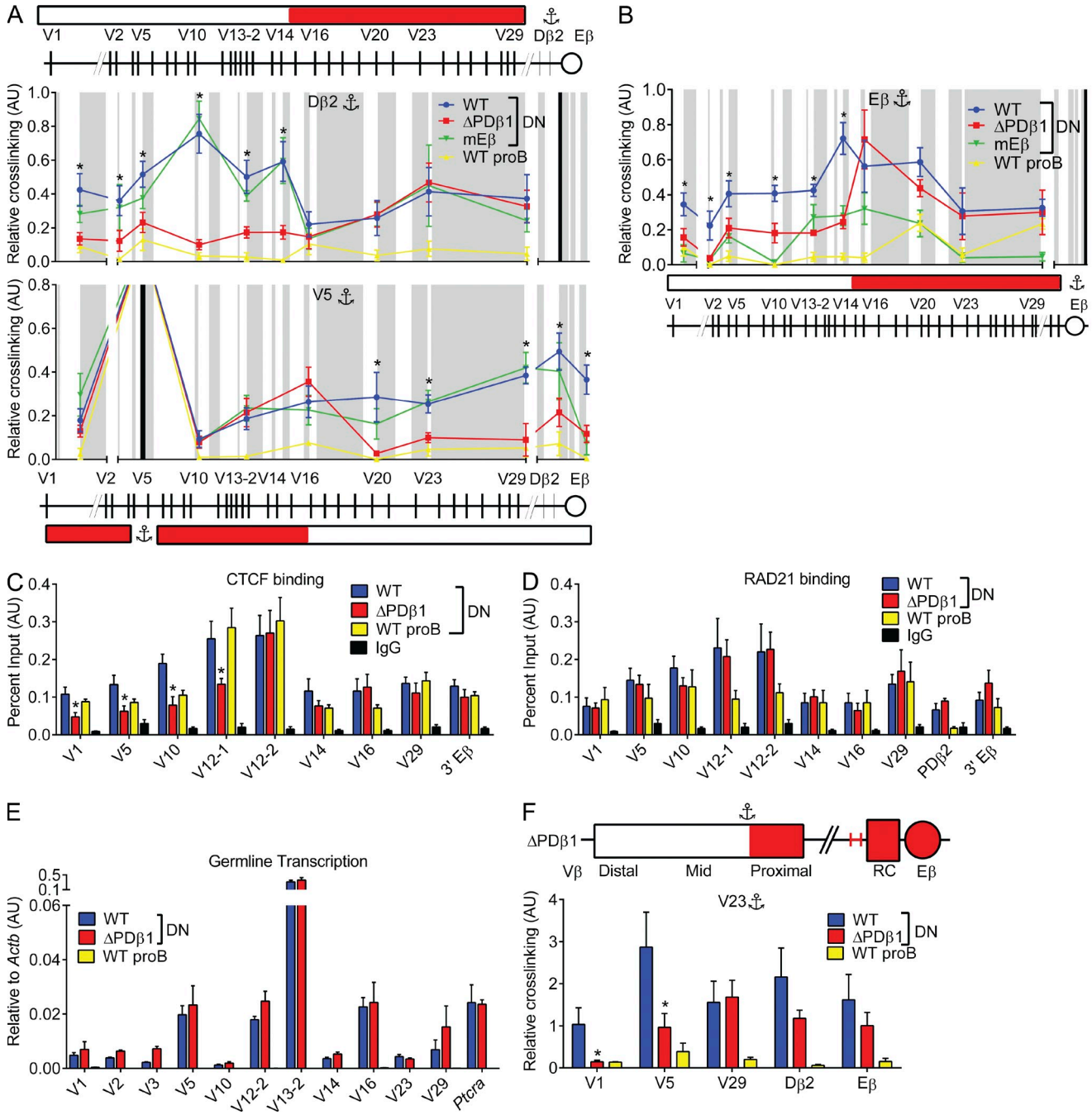

Figure 3. Deletion of the 5′RC flank resolves two *Trbv* interaction domains. (A and B) 3C analysis of RAG-deficient thymocytes (WT, ΔPDβ1, or mEβ alleles) and pro-B cells using the Dβ2 (A, top), *Trbv5* (A, bottom), and Eβ (B) viewpoints (anchors). Individual HindIII fragments are represented by alternating white and gray bars. Bold black bars indicate viewpoint locations. Schematics of *Tcrb* are shown on top and below primary 3C data, which are presented as mean values (±SEM) from at least three independent experiments. Thymocytes were pooled from 5–10 mice per 3C experiment. Significant differences between WT and ΔPDβ1 samples are denoted as *, $P < 0.05$ (Student's *t* test). See Fig. 1 for details of cartoon data summaries. Here, red shading indicates that *Trbv*-Dβ2 cross-linking in ΔPDb1 relative to WT alleles was unchanged (darkest red) or reduced to background levels in pro-B cells (white). (C and D) ChIP-qPCR assay for CTCF (C) and RAD21 (D) binding at sites near the indicated *Trbv* segments. Refer to Fig. 2 C for details. Data are presented as mean percent input (±SEM) with thymocytes pooled from at least 5–10 mice per experiment. (E) *Trbv* germline transcription was quantified relative to *Actb* by qRT-PCR from at least three independent experiments (involving one to three mice per experiment). Data are presented as mean relative expression (±SEM). Statistically significant differences are denoted as *, $P < 0.05$ (Student's *t* test). (F) 3C assays were performed with the *Trbv23* viewpoint (anchor). Schematic of *Tcrb* is shown on top. Data are presented as mean relative cross-linking (±SEM). Statistically significant differences between WT and ΔPDβ1 are denoted as *, $P < 0.05$ (Student's *t* test).

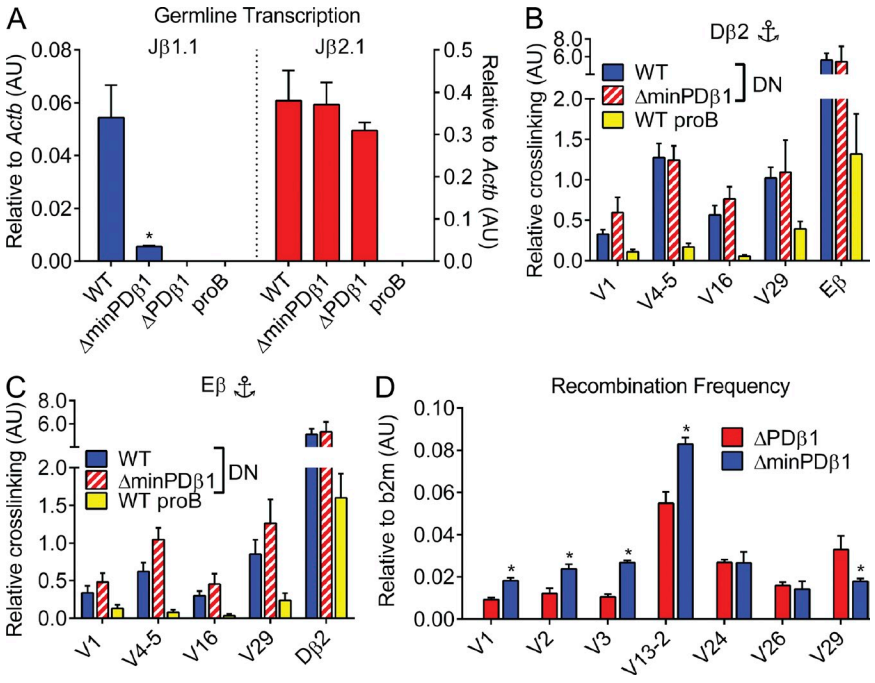

Figure 4. *Tcrb* looping is independent of Dβ1 promoter function. (A) Spliced germline transcripts traversing Jβ1.1 or Jβ2.1 to their respective Cβ exons were quantified relative to *Actb* (using RT-qPCR) in DN thymocytes from the indicated genotypes and WT pro-B cells (one to three mice). (B and C) 3C assays were performed with Dβ2 (B) and Eβ (C) viewpoints (anchors) in the indicated genotypes. Thymocytes were pooled from 5–10 mice for each 3C assay. (D) Quantification of *Trbv* usage in total thymocytes from ΔPDβ1 and ΔminPDβ1 mice on a RAG-sufficient background (recombination frequency). Relative levels of joins between the indicated Vβ segments and Dβ2Jβ2.1 were assayed and normalized as described previously (Gopalakrishnan et al., 2013). Data are represented as mean of three independent experiments involving individual mice (±SEM) with statistically significant differences indicated as *, $P < 0.05$ (Student's *t* test).

from ΔminPDβ1/*Rag1*$^{-/-}$ mice (Fig. 4 A; Whitehurst et al., 2000). Despite this dramatic transcriptional defect, long-range *Trbv*-RC interactions are unaffected by the ΔminPDβ1 deletion (Fig. 4, B and C).

Together, these data indicate that the *Trbv* array is topologically divided into two domains. The more proximal half of *Trbv*, which still lies >250 kb upstream of the DβJβ clusters, associates with the RC in thymocytes via mechanisms that are independent of PDβ1 and Eβ. The distal half of *Trbv* forms tissue-specific contacts with both the RC and the proximal *Trbv* domain. Although these interactions are independent of PDβ1 promoter activity, they require a 3-kb region upstream of this minimal control element. Importantly, we find that the most distal *Trbv* segments are significantly underutilized in Vβ-Dβ2Jβ rearrangements when comparing ΔPDβ1 with ΔminPDβ1 thymocytes on RAG-sufficient backgrounds (Fig. 4 D). In contrast, *Trbv* segments in the proximal domain are used at comparable or higher frequencies in ΔPDβ1 thymocytes. Thus, mechanisms that ensure tethering of distal *Trbv* domains are important for generating maximal diversity in the TCRβ repertoire.

Tcrb contraction is PDβ1 dependent but Eβ independent

Tcrb undergoes a large-scale spatial reconfiguration, termed contraction, upon differentiation of progenitors into DN thymocytes (Skok et al., 2007). As monitored by 3D fluorescent in situ hybridization (FISH), contraction brings opposing termini of *Tcrb*, the distal 5′ *Trbv* region and RC, into proximity, to facilitate long-range V-DJ recombination. Upon assembly of a productive *Tcrb* allele and transition to the double-positive (DP) stage of development, locus contraction is reversed, segregating the *Trbv* and DJ clusters, presumably enforcing allelic exclusion (Skok et al., 2007). However, functional relationships between AgR locus contraction and long-range V-RC looping remain unclear.

To test whether known REs contribute to *Tcrb* contraction, we performed 3D-FISH analyses on thymocytes from RAG-deficient mice harboring WT, mEβ, and ΔPDβ1 alleles. RAG1$^{-/-}$:D708A thymocytes were also assayed to test whether the deposition of RAG1 influences *Tcrb* contraction. Representative primary data for FISH experiments are shown in Fig. 5 A. As expected, distances between the V1 and trypsinogen probes (Fig. 5 B, top) are significantly greater in *Rag1*$^{-/-}$ DP versus DN thymocytes, reflecting the contracted nature of *Tcrb* in the latter (Fig. 5 B, bottom). *Tcrb* contraction is unaffected in DN thymocytes upon inactivation of the RC (mEβ and ΔEβ thymocytes), RAG1:D708A binding, or loss of the minimal Dβ1 promoter (Fig. 5 B). In contrast, the locus adopts an intermediate conformation in ΔPDβ1/*Rag1*$^{-/-}$ thymocytes, significantly more extended than in DN cells harboring a WT-*Tcrb* but significantly more contracted than in their DP counterparts.

These conclusions are supported by FISH data using two additional probe sets that measure distances between the RC and either the most distal *Trbv* segment (*Trbv1*; Fig. 5 C) or the main portion of the distal domain (*Trbv2-12*; Fig. 5 D). Thus, consistent with 3C data, folding of the most distal *Trbv* portion into the RC-3′*Trbv* aggregate is independent of transcriptional activity at DβJβ clusters. Instead, full contraction of the locus requires a region directly upstream of the RC, which includes PDβ1.

A CTCF-binding region serves as the focal point for distal *Trbv*–RC interactions

In an attempt to understand how the region upstream of minPDβ1 impacts long-range *Tcrb* looping, we surveyed its

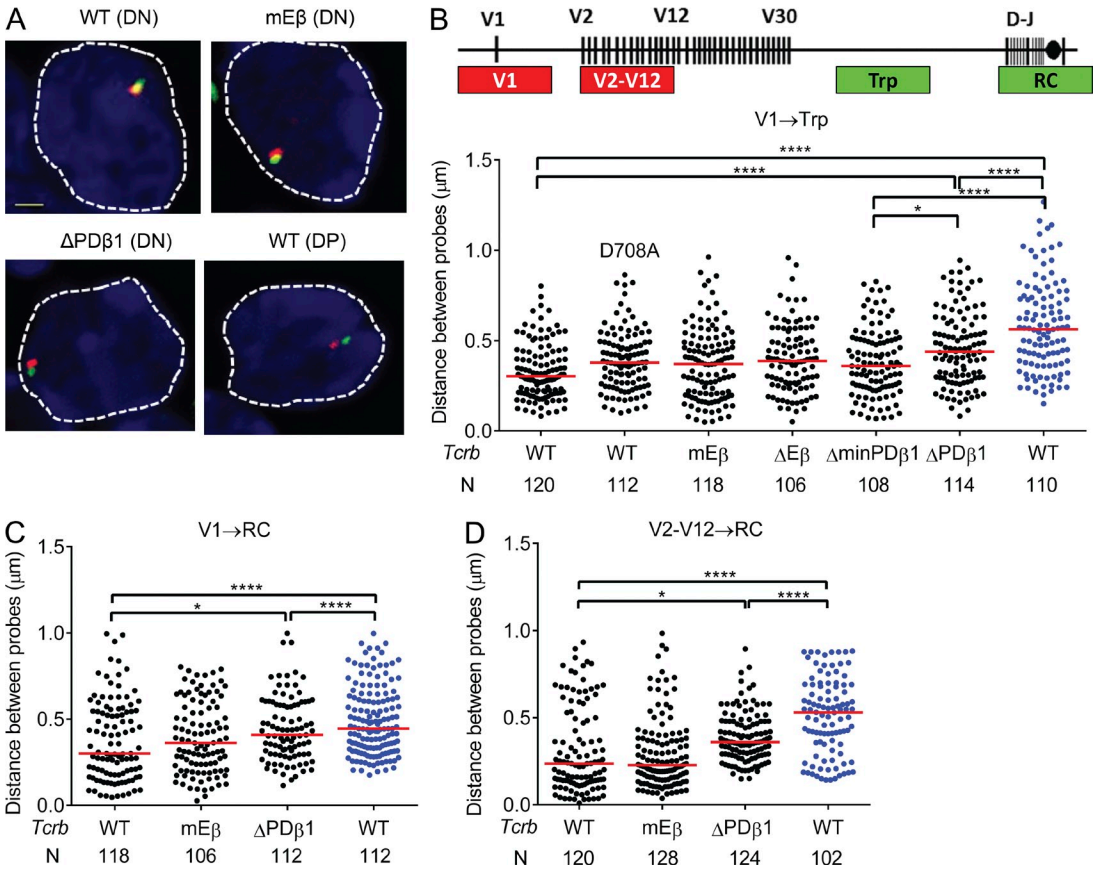

Figure 5. Partial decontraction of the *Tcrb* locus in ΔPDβ1 thymocytes. (A) Representative confocal 3D-FISH images of *Tcrb* locus contraction for the V1 (red) and trypsinogen region BAC probes (green) quantified in B. Blue corresponds to DAPI staining. Nuclear delimitation is indicated with dashed white lines. Bar, 1 µm. (B–D) Distances between the indicated regions of *Tcrb* were measured from 3D-FISH images as in A using BAC probes spanning *Trbv1* (red) and trypsinogen (green; B), *Trbv1* and the RC (green; C), and *Trbv2-12* (red) and the RC (green; D). Contraction was measured in RAG-deficient DN thymocytes (shown as black dots) for the indicated *Tcrb* genotypes or in DP thymocytes (blue dots). Results are presented as scatter plots of distances between probe foci for each *Tcrb* allele and represent total data from at least three independent preparations of slides. Thymocytes were pooled from 5–10 mice for each slide preparation. Statistical analyses revealed no significant differences between independent experiments performed on the same genotype or cell type. Median values are indicated by red horizontal lines. N represents the total number of foci analyzed by 3D-FISH for each genotype and probe set. Significant differences are denoted as *, $P \leq 0.05$; and ****, $P \leq 0.0001$ (one-way ANOVA, Tukey's post hoc test).

interactions with a distal portion of the *Trbv* cluster. Using *Trbv5* as a viewpoint, we scanned interactions with a series of restriction fragments upstream of PDβ1 (Fig. 6 A). Compared with pro-B cells, *Trbv5* cross-links more efficiently with this region in DN thymocytes at nearly all tested locations. The most robust *Trbv5* interaction occurs upstream of a silent trypsinogen gene, termed *Prss2*, which coincides with a prominent site for CTCF binding (Fig. 6 A, bottom; Shih et al., 2012). Association between *Trbv5* and this region, which we call the 5′*Prss2*-CTCF site (5′PC), is even greater than its interaction with the RC. Importantly, this prominent contact is disrupted in *Tcrb* loci with the large (ΔPDβ1), but not the minimal, Dβ1 promoter deletion. These findings are completely consistent with 3C data obtained with either 5′PC (Fig. 6 B) or two other distal *Trbv* segments as viewpoints for interactome analyses (Fig. 6, C and D). In contrast, robust interactions between 5′PC and proximal *Trbv* segments are unaffected by the ΔPDβ1 deletion (Fig. 6 E). We conclude that 5′PC is a focal point for long-range interactions between the distal *Trbv* domain and the RC, a process which depends on a region upstream of minimal PDβ1.

An RC barrier element is required for long-range *Trbv* looping to 5′PC

Although 5′PC tethers the distal *Trbv* domain, the mechanisms by which ΔPDβ1, but not ΔminPDβ1, disrupts thymocyte-specific contacts were unclear. In this regard, the 5′PC region remains completely intact on ΔPDβ1 alleles; deleted sequences are restricted to a region at least 20 kb downstream (Fig. 6 A, bottom). Furthermore, chromatin immunoprecipitation (ChIP) experiments reveal no significant differences in CTCF or RAD21 binding at 5′PC when comparing WT and ΔPDβ1 alleles (Fig. 6 F). These findings imply that an activity associated with the 3-kb region upstream of minPDβ1 impacts the ability of 5′PC to form long-range interactions with distal portions of *Trbv*.

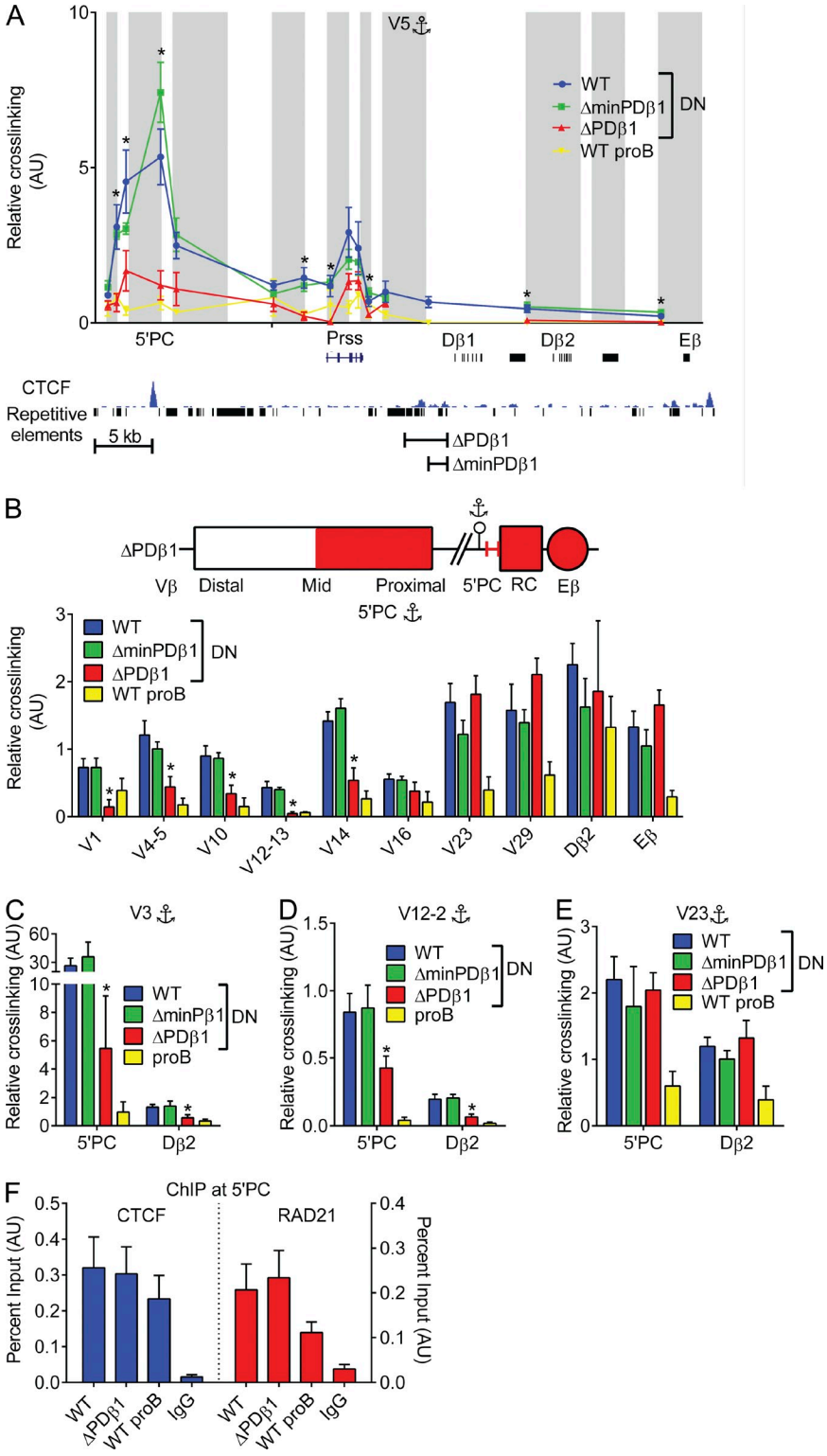

Figure 6. Identification of a *Trbv* tethering point in the RC flank. (A–E) 3C data for *Trbv5* (A; the bottom shows ChIP-seq track for CTCF in DN thymocytes [Shih et al., 2012] as well as locations of repetitive elements), 5′PC (B; schematic shown on top for 5′PC viewpoint; see Fig. 1 E), *Trbv3* (C), *Trbv12-2* (D), and *Trbv23* (E) viewpoints (anchors) in RAG-deficient DN thymocytes (WT, ΔPDβ1, or ΔminPDβ1 mice) or pro-B cells (see Fig. 1 A for details). (F) ChIP-qPCR for CTCF and RAD21 at 5′PC in the indicated cell types. All data are represented as means (±SEM) of three independent experiments. Thymocytes were pooled from 5–10 mice for each 3C or ChIP assay. Significant differences are denoted as *, $P \leq 0.05$ (Student's *t* test between WT and ΔPDβ1 genotypes).

The region of interest has several distinguishing characteristics, including a repetitive tract at its 5′ end and a pair of low-intensity CTCF/RAD21-binding sites (Fig. 6 A, bottom). These features are reminiscent of insulators that form boundaries between active and repressive chromatin domains (Wendt et al., 2008). In keeping with this possibility, a gene situated upstream of the putative chromatin barrier, *Prss2*, is transcriptionally active in ΔPDβ1 thymocytes but is completely silent in the context of WT, ΔminPDβ1, or mEβ alleles (Fig. 7 A). *Prss2* activation in ΔPDβ1 thymocytes is

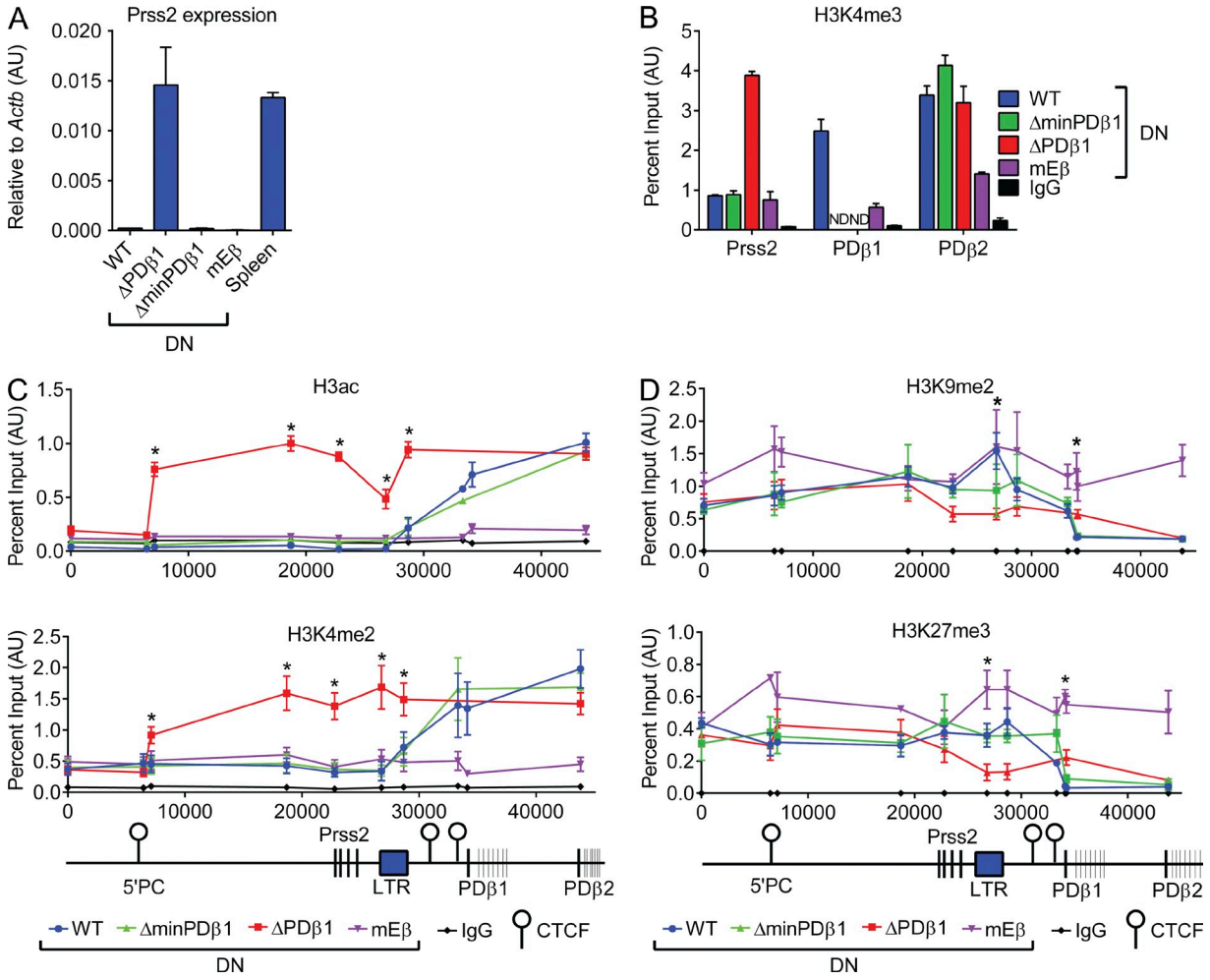

Figure 7. Long-range *Trbv* looping to 5′PC requires an RC barrier element. (A) Expression of *Prss2* transcripts were measured by RT-qPCR relative to *Actb* in DN thymocytes (WT, ΔPDβ1, ΔminPDβ1, and mEβ mice) and in spleen from C57BL/6 mice (positive control). (B–D) ChIP-qPCR assays were performed in DN thymocytes from RAG1$^{-/-}$ mice in the indicated *Tcrb* genotypes. Shown are levels of the H3K4me3 modification at the indicated promoters (B), as well as levels for active histone marks H3ac (C, top) and H3K4me2 (C, bottom) and repressive histone marks H3K9me2 (D, top) and H3K27me3 (D, bottom) at the indicated sites upstream or within the RC. All data are represented as means (±SEM) of at least two independent experiments. Thymocytes were pooled from four to eight mice for each experiment. Significant differences between only the WT and ΔPDβ1 genotypes are denoted as *, $P \leq 0.05$ (Student's *t* test).

mirrored by an acquisition of H3K4me3 at its promoter region (Fig. 7 B).

To further define how the ΔPDβ1 deletion impacts neighboring chromatin domains, we performed ChIP experiments for activating histone modifications within and upstream of the *Tcrb*-RC. As shown in Fig. 7 C (bottom), the H3K4me2 mark for accessible chromatin spreads throughout the RC in DN thymocytes, continuing to a CTCF site upstream of minPDβ1, after which it drops dramatically (Carabana et al., 2011). As expected, this modification is nearly absent in mEβ thymocytes, which harbor inactive *Tcrb*-RCs. Strikingly, H3K4me2 spreads much further upstream in thymocytes from the ΔPDβ1, but not ΔminPDβ1 mice, indicating disruption of a chromatin boundary in the former. Instead, a new chromatin boundary is established at or near 5′PC in the ΔPDβ1 thymocytes. A similar profile is observed for a second active chromatin mark, H3ac (Fig. 7 C, top).

Conversely, the repressive modifications H3K9me2 and H3K27me3, drop significantly near the boundary region upstream of the RC in DN thymocytes with either WT or ΔminPDβ1 alleles (Fig. 7 D). When enhancer function is disrupted (mEβ), the H3K9me2 and K3K27me3 marks also cover the inactivated RC, as expected. When the border region is removed (ΔPDβ1), there is a modest, but significant loss of these modifications directly upstream, likely reflecting the invasion of active chromatin into this normally repressed region. Similarly, there is a modest invasion of the two repressive marks into the most proximal end of the RC. Thus, the most significant impact of removing the 5′PDβ1 boundary region is the invasion of active chromatin (H3K4me2 and

H3ac) for a substantial distance upstream of the RC, resulting in the transcriptional activation of *Prss2*.

Collectively, our results demonstrate that the region upstream of PDβ1 serves as a chromatin barrier, which is required to preserve the function of 5′PC as a tether for distal regions of the *Trbv* cluster. When the normal boundary separating active from inactive chromatin is disrupted by the ΔPDβ1 deletion, a barrier function for 5′PC is unmasked, impairing its ability to maintain distal *Trbv*-RC contacts.

DISCUSSION

Lineage- and stage-specific assembly of AgR genes requires whole-scale changes in locus structure and extensive revisions to their chromatin landscapes, which are largely directed by regulatory elements flanking RCs. Here, we shed light on the complex function of these regulatory elements in both aspects of *Tcrb* assembly. As discussed below, our findings have implications not only for regulatory strategies used by other AgR loci, but also for the spatial mechanisms that control gene expression programs.

Tcrb adopts a thymocyte-specific conformation that, surprisingly, is independent of RC activity, including its transcription and binding of RAG proteins. Instead, the fully active *Tcrb* conformation requires a region directly flanking the RC, which functions as a barrier element to block the spread of active RC chromatin into a repressive upstream region. Disruption of the barrier relocates the active–inactive chromatin boundary to the nearest upstream CTCF site (5′PC), which normally serves as a major tethering point for distal *Trbv* segments. Our findings suggest that forcing 5′PC to become an insulator decommissions its tethering function, partially unspools the active *Tcrb* conformation, and skews the primary repertoire to favor more proximal *Trbv* segments.

Although Eβ function is essential for RC activation, it is dispensable for long-range association between *Trbv* segments and the two DβJβ clusters. Similarly, *Tcrb* contraction is Eβ independent, an observation which is consistent with data from other AgR loci harboring enhancer deletions (Shih and Krangel, 2013). These findings preclude several proposed mechanisms for the folding of AgR loci, or at least *Tcrb*, into their active conformations, including (a) a requirement for accessible RC chromatin, (b) RAG-mediated interactions between RC and V domains, and (c) co-occupancy of the RC and distal V segments in a transcription factory. Instead, we find that the crippled enhancer either protrudes from the Vβ–DβJβ interactome or is potentially sequestered into the central *Trbv12-16* gene cluster, resulting in transcriptional attenuation of the most active *Trbv* segments. Suppression of these *Trbv* segments is unlikely to result directly from loss of enhancer contact, but rather is an indirect effect of their continued association with a repressed RC. In support of this possibility, contacts between many of these Vβ segments and the RC are disrupted on the ΔPDβ allele, which retains robust expression of the Dβ2Jβ cluster, as well as a normal level of germline Vβ transcription. Likely, germline transcription of the *Trbv* segments is mostly caused by the activity of their associated promoters, but when juxtaposed with a repressive chromatin environment in the mEβ alleles, the promoters are silenced.

The general relevance of enhancer-independent V-RC association at other AgR loci is uncertain given available data, in part because *Ig* loci, unlike *Tcrb*, are decorated with multiple enhancers that form interaction networks and could have redundant functions in generating an active conformation (Degner-Leisso and Feeney, 2010). Of equal importance, many of the prior studies have probed locus-wide interactions only from the enhancer perspective, but based on our findings, viewpoints within the (D)J cluster itself may yield more relevant data for long-range V-RC interactions (Guo et al., 2011a; Medvedovic et al., 2013). At *Tcra*, a single enhancer (Eα) is tethered to the Jα germline promoter (TEA), generating an active chromatin hub for tertiary interactions with proximal *Trav* segments (Shih et al., 2012). Deletion of either Eα or TEA perturbs the proximal Vα to Jα contacts or redistributes enhancer interactions to include the intervening *Tcrd* locus. Thus, in contrast to *Tcrb*, interactions between proximal V segments and their RC targets are enhancer dependent at *Tcra*, suggesting that certain aspects of topological control are AgR locus specific. Conformational requirements likely are tailored to the unique architectures of *Ig* and *Tcr* loci and may reflect the broad range of spatial mechanisms that can be used to control gene expression in eukaryotes.

A surprising aspect of our study was that removal of the 5′RC flank, which includes PDβ1, disrupts long-range *Tcrb* interactions, resolving the *Trbv* cluster into distal and proximal domains, each with unique spatial determinants. The bidomainal architecture of *Trbv* is apparent from effects of the ΔPDβ1 deletion on long-range associations in a cell population (3C assays) or by probing locus contraction in single cells (3D-FISH). The protrusion of distal *Trbv* segments from the Vβ–DβJβ interactome is independent of promoter function because a more specific disruption of the core PDβ1 element has no impact on distal *Trbv*-RC juxtaposition. Based on our extensive 3C data, we map the approximate border between proximal and distal Vβ interaction domains to within the *Trbv14-16* region, a 16-kb stretch. Although precise border mapping and underlying mechanisms for its establishment remain to be resolved, we point out that the boundary coincides well with a transition between robust CTCF binding within the distal *Trbv* portion and more modest binding of these structural factors in the proximal domain (Fig. 2 C; Shih et al., 2012). We have been unable to identify other distinguishing characteristics of this region, including unique chromatin landscapes or predicted transcription factor sites. In what may be a related issue, determinants for tethering the proximal *Trbv* domain to its RC target, 250 kb away, remain unknown. Like the distal domain, proximal *Trbv* segments form major contacts with 5′PC; however, these interactions are unaffected by the ΔPDβ1 deletion. In contrast with the distal domain, proximal *Trbv* segments generally form equally robust associations with 5′PC and the RC. Based on these observations, we propose that the distal *Trbv* cluster relies on CTCF-dominant contacts with 5′PC to bring it into proximity with

the RC. Disruption of these contacts may also explain the partial loss of CTCF binding near distal *Trbv* segments in ΔPDβ1 thymocytes. In contrast, the proximal region of *Trbv* could also bridge to the RC by CTCF-independent mechanisms, which may be analogous to transcription factor–mediated looping at *Igh* (Medvedovic et al., 2013).

In our quest to decipher how the 5′RC flank impacts its association with distal *Trbv* segments, we found that the ΔPDβ1 deletion disrupts a chromatin boundary. As a result, hyperactive RC chromatin spreads upstream, leading to inappropriate expression of the silent *Prss2* gene. Although the deleted region exhibits two modest peaks of CTCF–RAD21 in DN thymocytes, the precise determinants of its insulator function remain unclear. In this regard, the region between PDβ1 and *Prss2* is repetitive and contains a viral LTR element that is expressed at low levels in DN thymocytes and has insulator properties (Carabana et al., 2011). A closer inspection of chromatin data for this region suggests that it contains a bimodal insulator consisting of the LTR, which blocks the spread of repressive chromatin downstream into the RC (Carabana et al., 2011), and the PDβ1-associated CTCF sites, which prevents the spread of hyperactive RC chromatin upstream into the *Prss2* region (shown here).

Notwithstanding these mechanistic uncertainties, deletion of the 5′RC flank disrupts an active chromatin barrier, which allows it to spread upstream until reaching the next CTCF region, 5′PC. When 5′PC becomes the dominant RC chromatin barrier, it is decommissioned as a long-range tether for distal *Trbv* segments. Several potential underlying mechanisms for this functional switch can be envisioned, including the major revision of local epigenetic landscapes when the RC-flanking insulator is disarmed. In this regard, cohesin mediates long-range chromatin looping not only through its association with CTCF, but also when it is recruited to the transcriptional mediator complex (Kagey et al., 2010). Emerging studies indicate that CTCF–cohesin bridges are predominantly structural in nature, similar to distal *Trbv*-5′PC interactions, whereas cohesin-mediator largely bridges loops between regulatory elements (Kagey et al., 2010). Perhaps the activation of transcription near 5′PC converts it into a region that favors participation in regulatory, rather than structural loops.

Our finding that distal *Trbv*-RC interactions depend on a bifunctional insulator-tethering element upstream of the RC is likely relevant to the architectural determinants of other AgR loci. For example, *Igh* enhancers interact with a CTCF-rich region, called the IGCR, which clearly serves as a chromatin boundary between its RC and proximal *Ighv* segments (Guo et al., 2011b). Similarly, two CTCF regions in *Igk*, termed Cer and Sis, contribute to the insulation of proximal *Igkv* segments from the enhancer-rich *Igkj* cluster (Xiang et al., 2011, 2013). Based on our discovery of a bifunctional element in the *Tcrb*-RC flank, we would hypothesize that at *Ig* loci, the most RC-proximal CTCF site or sites serve as an insulator (e.g., CBE2 in IGCR; Sis at *Igk*) to protect the tethering function of the more distal CTCF site or sites (e.g., CBE1 in IGCR; Cer at *Igk*). Resolution of these issues in the topological regulation of AgR loci will lend important insights into the menu of mechanisms that can be deployed to control gene expression programs in response to developmental cues or physiological agonists.

MATERIALS AND METHODS

Mouse strains. ΔPDβ1, ΔEβ, and ΔminPDβ1 mice were maintained on a Rag1$^{-/-}$/C57BL/6 background (Bories et al., 1996; Whitehurst et al., 2000). DP thymocytes were generated in *Rag1*$^{-/-}$ mice by anti-CD3ε injections as described previously (Shinkai and Alt, 1994). The mEβ mouse, which harbors crippling mutations at both Runx-binding sites in Eβ, was generated by homologous recombination in embryonic stem cells. In brief, the endogenous Runx-binding sequences TGTGGTT and TGCCACA in Eβ were mutated to TGTCCAT and TTGGACA, respectively. The mEβ allele was backcrossed onto the Rag1$^{-/-}$/C57BL/6 background. D708A mice were obtained from the Schatz laboratory (Ji et al., 2010b). Rag1$^{-/-}$/C57BL/6 mice were used as positive control for 3C, ChIP, and germline transcription assays and are labeled as WT in the figures. Developmental stages in RAG-deficient thymocytes harboring different *Tcrb* genotypes were assessed by CD44:CD25 staining. The majority (>94%) of cells were DN3 in each of the genotypes, as expected (Yannoutsos et al., 2001). All animal procedures were approved by the Institutional Animal Care and Use Committee of Washington University School of Medicine in St. Louis.

Tissue isolation and cell sorting. Single cell suspensions of thymocytes from *Rag1*$^{-/-}$ mice of various *Tcrb* genotypes were used for 3C, ChIP, expression, and 3D-FISH experiments. CD19 microbeads (Miltenyi Biotec) were used to isolate pro-B cells from the bone marrow of *Rag1*$^{-/-}$ mice using an autoMACS Pro Separator (Miltenyi Biotec).

3C assays. 3C assays were performed and analyzed as described previously (Hagège et al., 2007; Gopalakrishnan et al., 2013). Refer to Tables S1 and S2 for primer and probe combinations.

ChIP. ChIP assays were performed as described previously (Gopalakrishnan et al., 2013). The following antibodies were used: CTCF (Rockland), Rad21 (Abcam), H3ac (EMD Millipore), H3K4me2 (Abcam), H3K4me3 (Abcam), H3K9me2 (Abcam), H3K27me3 (Abcam), and IgG (Santa Cruz Biotechnology, Inc.). ChIPs were analyzed by qPCR using SYBR Green and primer combinations shown in Table S3. The LTR region between *Prss2* and *Tcrb*-RC was assayed with primers 7.4 UDB and 5.5 UDB published previously (Carabana et al., 2011).

3D-FISH. Hybridizations were performed with bacterial artificial chromosomes (BACs) that recognize the *Trbv1* (RP23-75P5), *Trbv2-Trbv12* (RP23-306O13), trypsinogen region (RP23-203H5), and the *Tcrb*-RC (RP23-421M9). To generate probes, BACs were nick translated with biotin and digoxigenin using Roche kits. The FISH probes were hybridized to slides of fixed, permeabilized thymocytes and then incubated with anti-biotin (Jackson ImmunoResearch Laboratories, Inc.), anti-digoxigenin, and DAPI (Invitrogen) stains. Hybridized slides were imaged on an A1 confocal microscope using 100× objective with 2× digital zoom (Nikon) and analyzed using ImageJ (National Institutes of Health) to measure 3D distances between foci as described previously (Shih and Krangel, 2010).

Germline *Tcrb* transcription. cDNA generated from 2 µg total thymocyte or pro-B cell RNA (iScript supermix; Bio-Rad Laboratories) was analyzed by qPCR using the primer combinations provided in Table S3.

Recombination assays. Genomic DNA was extracted from 10^6 total thymocytes using the DNeasy Blood and Tissue kit (QIAGEN). TaqMan qPCR assays to measure Jβ2 rearrangement frequencies were performed as described previously (Gopalakrishnan et al., 2013).

Online supplemental material. Tables S1 and S2 show TaqMan probes and primers used for 3C-qPCR analysis, and Table S3 shows primers used

for ChIP and gene expression analysis by qPCR. Primers and probes were obtained from Sigma-Aldrich. Online supplemental material is available at http://www.jem.org/cgi/content/full/jem.20141479/DC1.

We would like to thank Drs. B. Sleckman and T. Egawa for their valuable comments. RAG D708A mice were kindly provided by Dr. David Schatz.

This research was supported by National Institutes of Health grants AI 079732 and AI 081224 to E.M. Oltz, AI 49934 to M.S. Krangel, AI 112621 to C.H. Bassing, and CA177086 to J.E. Horowitz, as well as a Leukemia and Lymphoma Society Scholar Award to C.H. Bassing.

The authors declare no competing financial interests.

Submitted: 4 August 2014
Accepted: 20 November 2014

REFERENCES

Bories, J.C., J. Demengeot, L. Davidson, and F.W. Alt. 1996. Gene-targeted deletion and replacement mutations of the T-cell receptor beta-chain enhancer: the role of enhancer elements in controlling V(D)J recombination accessibility. *Proc. Natl. Acad. Sci. USA*. 93:7871–7876. http://dx.doi.org/10.1073/pnas.93.15.7871

Bouvier, G., F. Watrin, M. Naspetti, C. Verthuy, P. Naquet, and P. Ferrier. 1996. Deletion of the mouse T-cell receptor beta gene enhancer blocks alphabeta T-cell development. *Proc. Natl. Acad. Sci. USA*. 93:7877–7881. http://dx.doi.org/10.1073/pnas.93.15.7877

Carabana, J., A. Watanabe, B. Hao, and M.S. Krangel. 2011. A barrier-type insulator forms a boundary between active and inactive chromatin at the murine TCRβ locus. *J. Immunol.* 186:3556–3562. http://dx.doi.org/10.4049/jimmunol.1003164

Cobb, R.M., K.J. Oestreich, O.A. Osipovich, and E.M. Oltz. 2006. Accessibility control of V(D)J recombination. *Adv. Immunol.* 91:45–109. http://dx.doi.org/10.1016/S0065-2776(06)91002-5

de Laat, W., and D. Duboule. 2013. Topology of mammalian developmental enhancers and their regulatory landscapes. *Nature*. 502:499–506. http://dx.doi.org/10.1038/nature12753

Degner-Leisso, S.C., and A.J. Feeney. 2010. Epigenetic and 3-dimensional regulation of V(D)J rearrangement of immunoglobulin genes. *Semin. Immunol.* 22:346–352. http://dx.doi.org/10.1016/j.smim.2010.08.002

Dekker, J., K. Rippe, M. Dekker, and N. Kleckner. 2002. Capturing chromosome conformation. *Science*. 295:1306–1311. http://dx.doi.org/10.1126/science.1067799

Gopalakrishnan, S., K. Majumder, A. Predeus, Y. Huang, O.I. Koues, J. Verma-Gaur, S. Loguercio, A.I. Su, A.J. Feeney, M.N. Artyomov, and E.M. Oltz. 2013. Unifying model for molecular determinants of the preselection Vβ repertoire. *Proc. Natl. Acad. Sci. USA*. 110:E3206–E3215. http://dx.doi.org/10.1073/pnas.1304048110

Guo, C., T. Gerasimova, H. Hao, I. Ivanova, T. Chakraborty, R. Selimyan, E.M. Oltz, and R. Sen. 2011a. Two forms of loops generate the chromatin conformation of the immunoglobulin heavy-chain gene locus. *Cell*. 147:332–343. http://dx.doi.org/10.1016/j.cell.2011.08.049

Guo, C., H.S. Yoon, A. Franklin, S. Jain, A. Ebert, H.-L. Cheng, E. Hansen, O. Despo, C. Bossen, C. Vettermann, et al. 2011b. CTCF-binding elements mediate control of V(D)J recombination. *Nature*. 477:424–430. http://dx.doi.org/10.1038/nature10495

Hagège, H., P. Klous, C. Braem, E. Splinter, J. Dekker, G. Cathala, W. de Laat, and T. Forné. 2007. Quantitative analysis of chromosome conformation capture assays (3C-qPCR). *Nat. Protoc.* 2:1722–1733. http://dx.doi.org/10.1038/nprot.2007.243

Hewitt, S.L., D. Farmer, K. Marszalek, E. Cadera, H.E. Liang, Y. Xu, M.S. Schlissel, and J.A. Skok. 2008. Association between the Igk and Igh immunoglobulin loci mediated by the 3′ Igk enhancer induces 'decontraction' of the Igh locus in pre-B cells. *Nat. Immunol.* 9:396–404. http://dx.doi.org/10.1038/ni1567

Jackson, A.M., and M.S. Krangel. 2006. Turning T-cell receptor beta recombination on and off: more questions than answers. *Immunol. Rev.* 209:129–141. http://dx.doi.org/10.1111/j.0105-2896.2006.00342.x

Jhunjhunwala, S., M.C. van Zelm, M.M. Peak, S. Cutchin, R. Riblet, J.J.M. van Dongen, F.G. Grosveld, T.A. Knoch, and C. Murre. 2008. The 3D structure of the immunoglobulin heavy-chain locus: implications for long-range genomic interactions. *Cell*. 133:265–279. http://dx.doi.org/10.1016/j.cell.2008.03.024

Ji, Y., A.J. Little, J.K. Banerjee, B. Hao, E.M. Oltz, M.S. Krangel, and D.G. Schatz. 2010a. Promoters, enhancers, and transcription target RAG1 binding during V(D)J recombination. *J. Exp. Med.* 207:2809–2816. http://dx.doi.org/10.1084/jem.20101136

Ji, Y., W. Resch, E. Corbett, A. Yamane, R. Casellas, and D.G. Schatz. 2010b. The in vivo pattern of binding of RAG1 and RAG2 to antigen receptor loci. *Cell*. 141:419–431. http://dx.doi.org/10.1016/j.cell.2010.03.010

Kagey, M.H., J.J. Newman, S. Bilodeau, Y. Zhan, D.A. Orlando, N.L. van Berkum, C.C. Ebmeier, J. Goossens, P.B. Rahl, S.S. Levine, et al. 2010. Mediator and cohesin connect gene expression and chromatin architecture. *Nature*. 467:430–435. http://dx.doi.org/10.1038/nature09380

Kosak, S.T., J.A. Skok, K.L. Medina, R. Riblet, M.M. Le Beau, A.G. Fisher, and H. Singh. 2002. Subnuclear compartmentalization of immunoglobulin loci during lymphocyte development. *Science*. 296:158–162. http://dx.doi.org/10.1126/science.1068768

Mathieu, N., W.M. Hempel, S. Spicuglia, C. Verthuy, and P. Ferrier. 2000. Chromatin remodeling by the T cell receptor (TCR)-β gene enhancer during early T cell development: Implications for the control of TCR-β locus recombination. *J. Exp. Med.* 192:625–636. http://dx.doi.org/10.1084/jem.192.5.625

Medvedovic, J., A. Ebert, H. Tagoh, I.M. Tamir, T.A. Schwickert, M. Novatchkova, Q. Sun, P.J. Huis In 't Veld, C. Guo, H.S. Yoon, et al. 2013. Flexible long-range loops in the VH gene region of the Igh locus facilitate the generation of a diverse antibody repertoire. *Immunity*. 39:229–244. http://dx.doi.org/10.1016/j.immuni.2013.08.011

Nasmyth, K., and C.H. Haering. 2009. Cohesin: its roles and mechanisms. *Annu. Rev. Genet.* 43:525–558. http://dx.doi.org/10.1146/annurev-genet-102108-134233

Oestreich, K.J., R.M. Cobb, S. Pierce, J. Chen, P. Ferrier, and E.M. Oltz. 2006. Regulation of TCRβ gene assembly by a promoter/enhancer holocomplex. *Immunity*. 24:381–391. http://dx.doi.org/10.1016/j.immuni.2006.02.009

Osipovich, O., and E.M. Oltz. 2010. Regulation of antigen receptor gene assembly by genetic-epigenetic crosstalk. *Semin. Immunol.* 22:313–322. http://dx.doi.org/10.1016/j.smim.2010.07.001

Osipovich, O., R.M. Cobb, K.J. Oestreich, S. Pierce, P. Ferrier, and E.M. Oltz. 2007. Essential function for SWI-SNF chromatin-remodeling complexes in the promoter-directed assembly of Tcrb genes. *Nat. Immunol.* 8:809–816. http://dx.doi.org/10.1038/ni1481

Phillips, J.E., and V.G. Corces. 2009. CTCF: master weaver of the genome. *Cell*. 137:1194–1211. http://dx.doi.org/10.1016/j.cell.2009.06.001

Ribeiro de Almeida, C., R. Stadhouders, M.J.W. de Bruijn, I.M. Bergen, S. Thongjuea, B. Lenhard, W. van Ijcken, F. Grosveld, N. Galjart, E. Soler, and R.W. Hendriks. 2011. The DNA-binding protein CTCF limits proximal Vκ recombination and restricts κ enhancer interactions to the immunoglobulin κ light chain locus. *Immunity*. 35:501–513. http://dx.doi.org/10.1016/j.immuni.2011.07.014

Sanyal, A., B.R. Lajoie, G. Jain, and J. Dekker. 2012. The long-range interaction landscape of gene promoters. *Nature*. 489:109–113. http://dx.doi.org/10.1038/nature11279

Schatz, D.G., and Y. Ji. 2011. Recombination centres and the orchestration of V(D)J recombination. *Nat. Rev. Immunol.* 11:251–263. http://dx.doi.org/10.1038/nri2941

Seitan, V.C., B. Hao, K. Tachibana-Konwalski, T. Lavagnolli, H. Mira-Bontenbal, K.E. Brown, G. Teng, T. Carroll, A. Terry, K. Horan, et al. 2011. A role for cohesin in T-cell-receptor rearrangement and thymocyte differentiation. *Nature*. 476:467–471. http://dx.doi.org/10.1038/nature10312

Shih, H.-Y., and M.S. Krangel. 2010. Distinct contracted conformations of the *Tcra/Tcrd* locus during *Tcra* and *Tcrd* recombination. *J. Exp. Med.* 207:1835–1841. http://dx.doi.org/10.1084/jem.20100772

Shih, H.-Y., and M.S. Krangel. 2013. Chromatin architecture, CCCTC-binding factor, and V(D)J recombination: managing long-distance relationships at antigen receptor loci. *J. Immunol.* 190:4915–4921. http://dx.doi.org/10.4049/jimmunol.1300218

Shih, H.-Y., J. Verma-Gaur, A. Torkamani, A.J. Feeney, N. Galjart, and M.S. Krangel. 2012. *Tcra* gene recombination is supported by a *Tcra*

enhancer- and CTCF-dependent chromatin hub. *Proc. Natl. Acad. Sci. USA*. 109:E3493–E3502. http://dx.doi.org/10.1073/pnas.1214131109

Shinkai, Y., and F.W. Alt. 1994. CD3 epsilon-mediated signals rescue the development of $CD4^+CD8^+$ thymocytes in RAG-$2^{-/-}$ mice in the absence of TCR β chain expression. *Int. Immunol.* 6:995–1001. http://dx.doi.org/10.1093/intimm/6.7.995

Sikes, M.L., R.J. Gomez, J. Song, and E.M. Oltz. 1998. A developmental stage-specific promoter directs germline transcription of D beta J beta gene segments in precursor T lymphocytes. *J. Immunol.* 161:1399–1405.

Sikes, M.L., A. Meade, R. Tripathi, M.S. Krangel, and E.M. Oltz. 2002. Regulation of V(D)J recombination: a dominant role for promoter positioning in gene segment accessibility. *Proc. Natl. Acad. Sci. USA*. 99:12309–12314. http://dx.doi.org/10.1073/pnas.182166699

Skok, J.A., R. Gisler, M. Novatchkova, D. Farmer, W. de Laat, and M. Busslinger. 2007. Reversible contraction by looping of the *Tcra* and *Tcrb* loci in rearranging thymocytes. *Nat. Immunol.* 8:378–387. http://dx.doi.org/10.1038/ni1448

Steinel, N.C., B.L. Brady, A.C. Carpenter, K.S. Yang-Iott, and C.H. Bassing. 2010. Posttranscriptional silencing of VβDJβCβ genes contributes to TCRβ allelic exclusion in mammalian lymphocytes. *J. Immunol.* 185:1055–1062. http://dx.doi.org/10.4049/jimmunol.0903099

Verma-Gaur, J., A. Torkamani, L. Schaffer, S.R. Head, N.J. Schork, and A.J. Feeney. 2012. Noncoding transcription within the Igh distal V(H) region at PAIR elements affects the 3D structure of the Igh locus in pro-B cells. *Proc. Natl. Acad. Sci. USA*. 109:17004–17009. http://dx.doi.org/10.1073/pnas.1208398109

Wendt, K.S., K. Yoshida, T. Itoh, M. Bando, B. Koch, E. Schirghuber, S. Tsutsumi, G. Nagae, K. Ishihara, T. Mishiro, et al. 2008. Cohesin mediates transcriptional insulation by CCCTC-binding factor. *Nature*. 451:796–801. http://dx.doi.org/10.1038/nature06634

Whitehurst, C.E., S. Chattopadhyay, and J. Chen. 1999. Control of V(D)J recombinational accessibility of the Dβ1 gene segment at the TCRβ locus by a germline promoter. *Immunity*. 10:313–322. http://dx.doi.org/10.1016/S1074-7613(00)80031-X

Whitehurst, C.E., M.S. Schlissel, and J. Chen. 2000. Deletion of germline promoter PDβ1 from the TCRβ locus causes hypermethylation that impairs Dβ1 recombination by multiple mechanisms. *Immunity*. 13:703–714. http://dx.doi.org/10.1016/S1074-7613(00)00069-8

Xiang, Y., X. Zhou, S.L. Hewitt, J.A. Skok, and W.T. Garrard. 2011. A multifunctional element in the mouse Igκ locus that specifies repertoire and Ig loci subnuclear location. *J. Immunol.* 186:5356–5366. http://dx.doi.org/10.4049/jimmunol.1003794

Xiang, Y., S.-K. Park, and W.T. Garrard. 2013. Vκ gene repertoire and locus contraction are specified by critical DNase I hypersensitive sites within the Vκ-Jκ intervening region. *J. Immunol.* 190:1819–1826. http://dx.doi.org/10.4049/jimmunol.1203127

Yannoutsos, N., P. Wilson, W. Yu, H.T. Chen, A. Nussenzweig, H. Petrie, and M.C. Nussenzweig. 2001. The role of recombination activating gene (RAG) reinduction in thymocyte development in vivo. *J. Exp. Med.* 194:471–480. http://dx.doi.org/10.1084/jem.194.4.471